Peer-reviewed version available at Sensors 2019, 19, 5313; doi:10.3390/s19235313

Article

Hydrogen Sensor Based on Tunable Diode Laser Absorption Spectroscopy

Viacheslav Avetisov [1,*], Ove Bjoroey [1], Junyang Wang [1,2], Peter Geiser [1] and Ketil Gorm Paulsen [1]

[1] NEO Monitors AS, Prost Stabels vei 22, 2019 Skedsmokorset, Norway;
viacheslav.avetisov@neomonitors.com (V.A.); ove.bjoroy@neomonitors.com (O.B.);
peter.geiser@neomonitors.com (P.G); ketil.paulsen@neomonitors.com (K.G.P.)
[2] Yinian Sensors Technology Co., Ltd, Shenzhen 518126, China junyang.wang@ecamana-tech.com (J.W.)
* Correspondence: viacheslav.avetisov@neomonitors.com

Abstract: A laser-based hydrogen (H_2) sensor using wavelength modulation spectroscopy (WMS) was developed for contactless measurements of molecular hydrogen. The sensor uses a distributed feedback (DFB) laser to target the H_2 quadrupole absorption line at 2121.8 nm. The H_2 absorption line exhibits weak collisional broadening and strong collisional narrowing effects. Both effects were investigated by comparing measurements of the absorption linewidth with detailed models using different line profiles that include collisional narrowing effects. The collisional broadening and narrowing parameters were determined for pure hydrogen as well as for hydrogen in nitrogen and air. Performance of the sensor was evaluated and the sensor applicability for H_2 measurements in a range of 0- 10 %v of H_2 was demonstrated. A precision of 0.02 %v was achieved with 1 meter of absorption pathlength (0.02 %v·m) and 1 s of integration time. For the optimum averaging time of 20 s a precision of 0.005 %v·m was achieved. A good linear relationship between H_2 concentration and the sensor response was observed. A simple and robust transmitter-receiver configuration of the sensor allows in-situ installations in harsh industrial environments.

Keywords: gas sensor; hydrogen sensor; diode laser; TDLAS; WMS; absorption spectroscopy; laser spectroscopy; hydrogen

1. Introduction

The increase in demand for hydrogen gas sensors is strongly coupled to the expanded use of hydrogen gas (H_2) in industry [1,2]. Hydrogen is an important feedstock in many industrial processes and applications including the oil & gas industry, chemical plants, the steel industry, to name a few. Refineries use hydrogen in a large number of operations, e.g. hydrotreating of various refinery process streams and hydrocracking of heavy hydrocarbons. Analyzing hydrogen in complex and varying gas mixtures is challenging and measurements are normally performed using gas chromatographs, which are accompanied by slow response times and high operational costs. Since hydrogen is highly flammable, strict regulations for using safety H_2 sensors apply. Many different types of safety hydrogen sensors are commercially available [3] and the common principle is a sensing element that is altered (e.g. resistance) when in contact with hydrogen. This mode of operation precludes the use of these point-type hydrogen sensors in reactive, corrosive and/or dusty gas streams. For this reason, contactless hydrogen sensing is highly desired. Diode lasers are extremely attractive for this purpose due to their inherently low intensity noise and narrow linewidth. These properties enable highly selective and sensitive probing of narrow and extremely weak H_2 absorption lines. As a diatomic homonuclear molecule, H_2 has no dipole moment that could create a strong optical absorption in the infrared region. The absorption spectrum of H_2 is therefore limited to vibrational bands of very weak electric quadrupole transitions [4], which is why laser-

based detection of H_2 so far have been limited to extractive cavity-enhanced sensors, based on cavity ring-down spectroscopy (CRDS) [5,6], intra-cavity output spectroscopy (ICOS) [7,8] and optical-feedback cavity-enhanced absorption spectroscopy (OF-CEAS) [9]. Common for these techniques is the confinement of the laser light in a high-finesse optical cavity by using a set of highly reflective mirrors. Up to several kilometers of effective absorption pathlength can be obtained, which allows for detection of very weak hydrogen quadrupole transitions. However, for use in industrial applications, where extremely high sample purity can be difficult to achieve, contamination of the mirrors is an issue. If not properly handled, this will lead to a degradation of the sensor sensitivity and can ultimately damage the coatings of the high reflectivity mirrors. For this reason, cavity-based H_2 sensors often impose rigid requirements on the gas sampling and conditioning systems and typically involve periodic maintenance.

Tunable Diode Laser Absorption Spectroscopy (TDLAS) [10,11] is a sensitive and selective method that directly probes the process (in-situ) without the necessity to extract gas samples. Gas sensors based on TDLAS are frequently used for many industrial process control, emission monitoring and safety applications and are well-accepted throughout many industries [12-16]. The underlying measurement principle is inherently contactless, and the instrumentation is consequently not exposed to potentially corrosive process gases. Concentration readings are made available in real-time, which is ideal for fast and efficient process control and safety-related measurements. Furthermore, in-situ measurements have low maintenance requirements and thus lower the operational costs. In general, compared to cavity-enhanced techniques TDLAS has lower complexity and is more robust, which has made TDLAS-based sensors the preferred platform for many industrial process control and safety applications.

We present in this paper the first laser-based infrared hydrogen absorption sensor for in-situ hydrogen measurements. The sensor can also be re-configured for extractive measurements for applications where an in-situ installation is not feasible due to e.g. high pressure and/or high temperature. Optical windows are isolating the process gas from the sensor so that the advantage of contactless measurements is maintained. The presented hydrogen sensor is based on the commercial LaserGas™ II platform [17] manufactured by NEO Monitors AS. The instrument was used to study a selected hydrogen absorption line in terms of line broadening and line narrowing effects. To validate the measurements, line shape modeling using different spectral line profiles was performed. The sensor showed a capability of measuring hydrogen with a precision of 0.02%v·m for 1 s of integration time, which is better than most intended safety applications require (assuming the measurement range of 0-10 %v). Using a response time of 1 second, an estimated limit of detection (LOD) for H_2 of 0.1 %v for 1 meter of absorption pathlength was achieved.

2. Sensor Design

The developed sensor follows the classical in-situ TDLAS design and consists of a transmitter and a receiver unit. The transmitter unit contains a diode laser, collimating optics, a microprocessor board and all input-output electronics. The transmitter unit also has a built-in cell for H_2 validation. The receiver unit incorporates a photodetector, focusing optics and signal detection electronics (amplifies, mixer etc.). Figure 1 shows a photograph of the LaserGas™ II sensor mounted on the demo pipe using the DN50 flanges.

Figure 1. TDLAS H_2 sensor mounted on a demo pipe. Transmitter unit is located to the left and the receiver unit to the right. The gas inlet and outlet of the validation build-in gas cell are indicated.

Peer-reviewed version available at Sensors 2019, 19, 5313; doi:10.3390/s19235313

The sensor is based on the wavelength modulation spectroscopy (WMS) technique, which is well described in the literature [18-20]. This technique has proven very useful in trace gas sensing due to its ability to perform very sensitive interference-free measurements directly in the process or across stack without sample extraction and preconditioning. Since WMS provides nominally baseline-free absorption signals it is especially suited for measurements of weak absorbances. Recently published comparisons of WMS and Direct Absorption Spectroscopy (DAS) techniques reveal that WMS is approximately one order of magnitude more sensitive [21-23]. Figure 2 shows a schematic diagram and basic principle of the sensor operation.

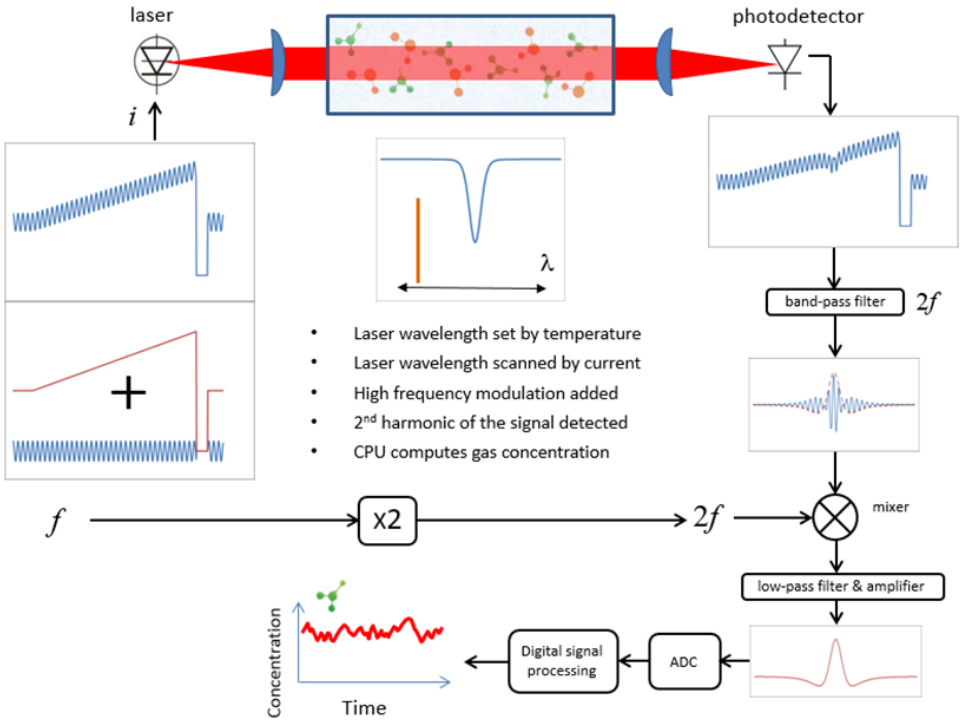

Figure 2. Schematic overview of the principles of the sensor operation. A sinusoidally modulated current ramp is applied to the laser, which is thereby swept in frequency across the transition of interest. After interaction with the sample the absorption information is encoded in the transmitted intensity, which is measured using a photodetector. The photodetector signal is amplified, filtered, mixed and digitized. Finally, digital signal processing is used to retrieve the concentration (and possibly other relevant parameters).

The temperature of the diode laser is stabilized with high accuracy (typically in the mK range) to set the average emission wavelength of the laser. A direct current (DC) is applied to operate the laser above its threshold, and a current ramp with a duration of 2 milliseconds is used to tune the wavelength over an absorption feature of interest. After each ramp the laser current is switched off for signal normalization purposes. In WMS, the laser current (and thus the emission wavelength of the laser) is modulated. For this purpose, a sinusoidal waveform of frequency f of about 100 kHz is added to the current ramp. The collimated laser beam is directed through the target gas, after which it is captured by the receiver optics and focused onto a photodetector. The signal detected by the photodetector is bandpass-filtered to select the $2f$ component and the filtered signal is detected using a hardware mixer, a low-pass filter and an amplifier. The $2f$ WMS signal is digitized using an AD converter and normalized to the measured direct signal. Before calculating the gas concentration additional digital signal processing can be applied to improve the signal-to-noise ratio (SNR) such as digital filtering, wavelet denoising, baseline fitting etc.

3. Line Selection

The absorption spectrum of H_2 in the infrared region is very sparse and extremely weak. Figure 3 shows a HITRAN simulation using default air broadening parameters listed in HITRAN16. The fundamental (1-0) vibrational electric-quadrupole transitions of H_2 are between 1900 and 3000 nm. There are only a few lines visible due to the large rotational constant that follows from the low mass of the H_2 molecule. The first overtone band (2-0) of H_2 is located between 1100 and 1500 nm. Compared to the fundamental band, the overtones have been studied much more extensively using cavity-enhanced spectrometers [6,24].

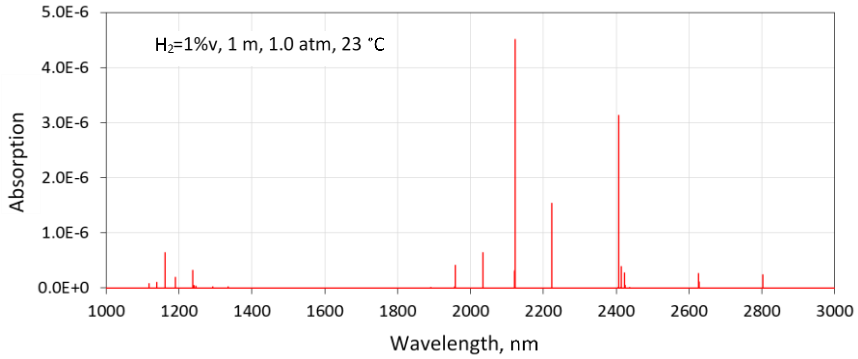

Figure 3. HITRAN simulation of H_2 absorption (1 %v·m) using default air broadening parameters listed in HITRAN16.

From the HITRAN simulations, three transitions in the fundamental vibrational band are identified as suitable for H_2 gas sensing: 2407 nm (4155.3 cm^{-1}), 2223 nm (4497.8 cm^{-1}) and 2122 nm (4712.9 cm^{-1}). However, the best available transition for industrial applications is not necessarily the strongest transition, but the one with least interference from gases such as water vapor (H_2O), carbon dioxide (CO_2), methane (CH_4), ammonia (NH_3), carbon monoxide (CO). The transition at 2407 nm is close to the strong H_2O absorption band at 2700 nm and several strong H_2O lines overlap with the weak H_2 line. Likewise, the transition at 2223 nm is suffering from strong NH_3 and CH_4 interferences, which would limit the industrial usage of a sensor that targets this transition. In addition, the strength of this line is about one third of the strength of the H_2 line at 2122 nm, which is the strongest H_2 line in the IR region. The line at 2122 nm is not completely free from CH_4 and NH_3 interference although it is much weaker than for the other mentioned H_2 lines. Also, CO_2 absorption in this spectral region must be considered due to potential interference. Since the linestrength is a crucial factor for sensing hydrogen the S(1) (1-0) line at 2121.8 nm (4712.9 cm^{-1}) was chosen. A DFB diode laser from Nanosystems and Technologies GmbH and an InGaAs pin photodetector from Hamamatsu were used in the sensor.

4. Experimental Results and Modelling of the H_2 Lineshape

The linestrength of the S(1) (1-0) H_2 transition is 3.2×10^{-26} cm/molecule [4]. Simulations using the air broadening parameter of 0.05 cm^{-1}/atm (default value listed in HITRAN16) and the Voigt profile indicates about 5×10^{-6} of relative peak absorbance for 1 %v H_2 over 1 meter of absorption pathlength (1 %v·m) under ambient conditions (Figure 3). Such absorbance is too weak for an in-situ absorption sensor that is required to detect sub-percent levels of H_2. However, predictions based on modelling using the Voigt profile are not correct. It is important to note that due to the low mass of the H_2 molecule, the Doppler broadening is significantly larger than what is typical for other molecules at this wavelength. The Doppler half width at half maximum (HWHM) for this transition is 0.0204 cm^{-1} at 296K and the small collisional cross-section and absence of dipole moment results in very weak collisional broadening while the high rate of velocity changing collisions contributes to an unusually

strong narrowing (the Dicke narrowing effect). The combination of these effects results in a line profile that deviates significantly from the Voigt profile. Hence, more advanced profiles must be used such as the Hartmann-Tran profile (HTP) [25] or other simpler profiles that include only the collisional narrowing such as Rautian profile (RP) [26] and Galatry profile (GP) [27]. Recently non-Voigt line profiles have been implemented in the HITRAN database [28] where HTP was explicitly recommended for modelling of the H_2 lines. However, by the time of writing, the non-Voigt line parameters for H_2 in air were not available in the HITRAN database. The line parameters used here for the S(1) (1-0) line for pure H_2 (self-broadening) were reported by P. Wcisło et.al. [28]. The reported the self-broadening parameter for this H_2 line was $\gamma_{self} = 0.0019$ cm^{-1}atm^{-1} and the velocity changing collision (narrowing) parameter was $\nu_{self}^{vc} = 0.0448$ cm^{-1}atm^{-1}. The combination of very weak self-broadening and strong narrowing should result in sub-Doppler widths of the H_2 line for pressures around ambient air pressure. Indeed, significant reduction of the H_2 linewidth with pressure and a corresponding increase of the peak amplitude has been reported for all studied H_2 lines in the overtone (2-0) vibrational band [6,24] for pure H_2 gas. However, nitrogen broadening, air broadening, and narrowing parameters have not yet been reported.

In this paper, we present the results of measurements of the self-broadening and narrowing parameters and the corresponding parameters for nitrogen and air for the S(1) (1-0) line. Since the laser intensity modulation amplitude, the modulation phase and the phase shift between the laser intensity and wavelength modulations all influence the shape of the 2*f*-WMS absorption signals, performing direct signal fitting using advanced line profiles with many fitting parameters can ambiguous. Such profile study requires good signal-to-noise ratio and exceptional precision of the recorded line profiles (better than 1% rel.), which is very challenging for the case of the weak H_2 transition. Therefore, another approach was chosen based on findings by J. Reid and D. Labrie [29] who investigated the behavior of the WMS lineshape as a function of the ratio between the modulation amplitude (a) and the absorption HWHM (Δ), $m = a/\Delta$. The WMS lineshapes for the Voigt profile and the limiting cases of the Voigt, the Gaussian and Lorentzian profiles were modelled. It was found that the peak amplitude of the WMS lineshape (WMS-PA) is maximized at $m = 2.2$ independent on the ratio of the collisional broadening to the Doppler broadening, i.e., whether the Voigt was in the Gaussian or Lorentzian regime. To find out if the same value of $m = 2.2$ is also valid for an absorption lineshape exhibiting strong collisional narrowing, we performed numerical simulations for HTP, RP and GP using the collisional broadening and narrowing parameters within the range of the values reported for different H_2 lines. In particular, we modelled the gas pressure region where collisional narrowing resulted in the most prominent effect on the H_2 lineshape: between 0.1 and 1.0 atm. The modelling shows that the calculated WMS signal, using any of these three profiles HTP, RP and GP plotted as functions of m, shows a peak at approximately the same value of $m = 2.2 \pm 0.1$. Figure 4 shows the result of the modelling of the S(1) (1-0) H_2 line using HTP and the line parameters for 100% H_2 gas by P. Wcisło et.al. [28]. The results for the Doppler profile were obtained by setting the H_2 pressure to $P = 0.01$ atm, which ensures that both collisional broadening and narrowing effects are negligible. The results for the Lorentzian profile were obtained by setting $P = 10$ atm, which ensures that both Doppler broadening and collisional narrowing are negligible. The plots for $P = 0.25$ atm and $P = 0.5$ atm represent the region where the collisional narrowing is significant. No significant difference between the WMS-PA m-dependence for HTP, RP and GP were found. This means that it is possible to indirectly measure the HWHM of an absorption line by varying the modulation amplitude of the laser while measuring the WMS-PA. Finally, the HWHM pressure dependence obtained from the measurements can be compared with the corresponding theoretical pressure dependence from the model. Such comparison provides a good estimation of the collisional broadening and narrowing coefficients (with an accuracy of the parameters determined by this method of about 10% rel.).

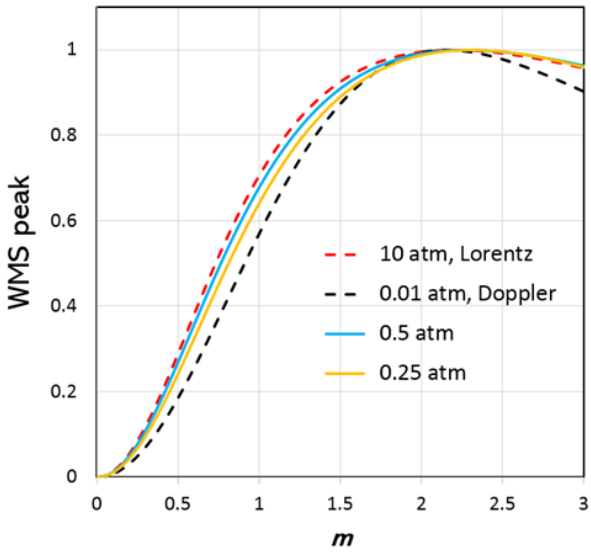

Figure 4. Calculated WMS peak amplitude (Hartmann-Tran profile) as a function of the normalized modulation amplitude, *m*, for H_2 at and 0.25 and 0.5 atm (100 % H_2) together with the Lorentzian limit at 10 atm, and the Doppler limit at 0.01 atm. The HTP line parameters for S(1) (1-0) H_2 transition given in [28] were used in the modelling.

To improve the SNR of the WMS-PA measurements the sensor was connected to a multi-pass cell of Herriott type with 12 meters pathlength, which was filled with pure H_2 gas at different pressures up to 4 atm. For measurements in nitrogen and air gas mixtures, pure hydrogen was diluted to 10 %v in the corresponding balance gas using a HOVAGAS gas mixer. The Doppler HWHM at 23°C of 0.204 cm^{-1} was used to calibrate the laser modulation amplitude *a* to the unit of cm^{-1} such that the experimentally obtained HWHM converges to the theoretical Doppler HWHM at zero pressure. The theoretical HWHM was obtained from the calculated HTP for different pressures. The results from the calculations were compared with the measured values and the broadening and narrowing coefficients used in the calculations were adjusted until the best fit with the measured results was achieved (ignoring line shift effects). Figure 5(a) shows the measured HWHM of the H_2 line for pure (100 %v) H_2 gas and the calculated HTP HWHM which resulted in the best fit. The parameters obtained are γ_{self} = 0.0024(3) $cm^{-1}atm^{-1}$ and ν_{self}^{vc} = 0.037(5) $cm^{-1}atm^{-1}$ (T=296 K). The parameters are in reasonable agreement with the values reported by P. Wcisło et.al.: 0.0019(1) and 0.0484, respectively (T=315 K) [28]. The parameter for broadening speed-dependence had negligible influence on the resulting pressure dependency of the HWHM. In the modelling this parameter was set to 1/10 of the broadening parameter and the correlation parameter was set to zero [4,28]. The calculated HWHM using RP and GP showed similar pressure dependence and the obtained broadening and narrowing parameters were the same as for HTP. Although accuracy of the experimental data did not allow to distinguish between HTP, RP and GP, the HTP results are presented in this study since this profile is particularly recommended for modelling of hydrogen absorption lines [28]. As seen in Figure 5(a), the absorption line of pure H_2 is extremely narrow (more than 2 times narrower than the Doppler HWHM) in a broad pressure range from around ambient up to several atm. The corresponding calculated HTP for a pressure of 1.0 atm is plotted in Figure 5(b) together with the corresponding Gaussian profile. The peak amplitude of the H_2 line (100%) at atmospheric pressure is more than a factor of 1.6 larger than if the H_2 line would be pure Gaussian with Doppler width.

Preprints (www.preprints.org) | NOT PEER-REVIEWED | Posted: 3 November 2019 doi:10.20944/preprints201911.0028.v1

Peer-reviewed version available at Sensors 2019, 19, 5313; doi:10.3390/s19235313

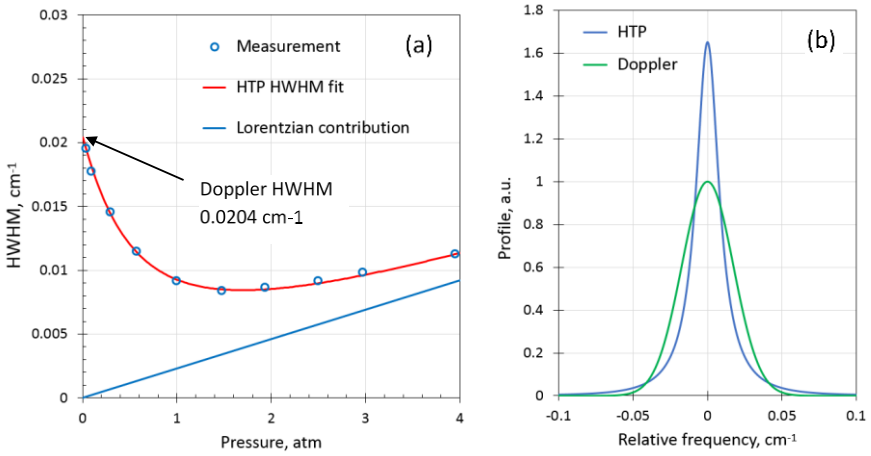

Figure 5. (a) The HWHM of H_2 100 %v as function of pressure together with a fit using the HTP; (b) the calculated HTP at P=1.0 atm compared to the corresponding Doppler Gaussian profile.

For gas sensing it is important to measure the collisional parameters (broadening and narrowing) in nitrogen and air balance. These parameters are not available in literature for the given H_2 transition. Figure 6(a) shows the pressure dependence of H_2 HWHM for 10% H_2 in nitrogen balance. Despite significantly larger nitrogen broadening compared to the self-broadening, the H_2 line in nitrogen around ambient pressures is narrower than the Doppler broadened line. In Figure 6(b) the modelled HTP at 1.0 atmosphere is compared with the Gaussian profile of the same integral. The peak amplitude of the H_2 line at 1 atm in nitrogen is 1.2 times larger than if the line would have only Doppler broadening. Using the previously obtained parameters for pure hydrogen, the collisional broadening and narrowing parameters for nitrogen balance were evaluated to be γ_{N2} = 0.0087(8) cm^{-1}atm^{-1} and ν_{N2}^{vc} = 0.071(7) cm^{-1}atm^{-1}, respectively (T=296K). Few measurements of H_2 in air balance at ambient pressure were made as well. The H_2 line appeared somewhat narrower than in nitrogen balance. It was assumed that the collisional narrowing parameter is the same as in nitrogen. The broadening coefficient in air was then estimated to be γ_{AIR} = 0.0081(8) cm^{-1}atm^{-1}.

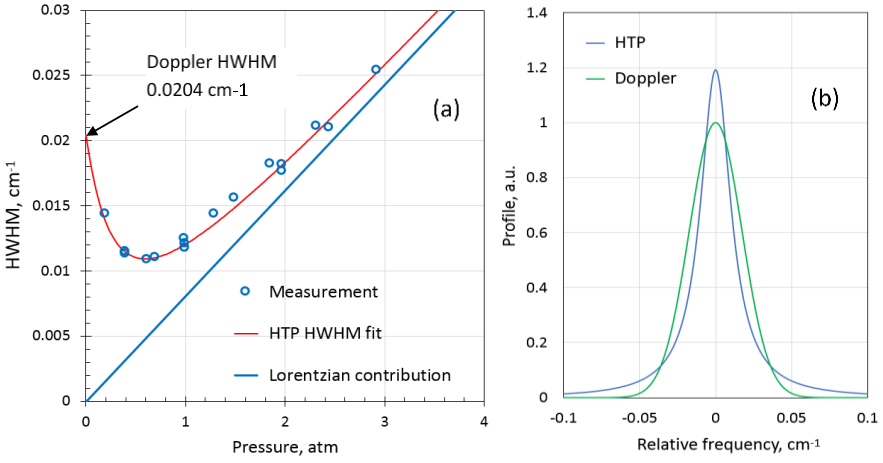

Figure 6. (a) The HWHM of 10 %v H_2 in N_2 balance gas as function of pressure and a fit using the HTP; (b) The calculated HTP at P=1.0 atm compared to the corresponding Doppler Gaussian profile.

5. H_2 Sensor Performance

The simulation using HTP with the linestrength listed in HITRAN and the collisional parameters obtained in this study for H_2 in nitrogen/air indicates that 1 %v H_2 over 1-meter optical pathlength (1 %v·m) gives about 2.2×10^{-5} of relative peak absorbance. This is about 4 times stronger absorbance than that calculated using the Voigt profile with the default HITRAN parameters (see Figure 1). To achieve the required LOD of 0.1-0.2 %v·m (assuming the measurement range of 0-10 %v) the sensitivity of the TDLAS sensor must be in the range of from 2 to 4×10^{-6} of the relative absorbance. The two main factors limiting the sensitivity of most TDLAS sensors is (*i*) optical fringe-noise, sometimes called etalon noise, which is interferences of the laser light caused by partially reflective surfaces in the system and (*ii*) coupling of stray light into to the laser active area (laser feedback noise). Considerable effort was put in the optomechanical design of the H_2 sensor to eliminate most sources of optical feedback and etalon noise. In addition, the modulation amplitude was carefully optimized for the very narrow H_2 line. A noteworthy biproduct of the relatively weak laser current modulation is that the residual amplitude modulation that contributes to the baseline variations in the WMS signal [30] was negligible.

For evaluation of the sensor performance the transmitter and receiver were set 1 meter apart on a test bench. A single-pass optical cell of 0.7 meter fitted with wedged windows was placed in between the transmitter and receiver. Different concentrations of H_2 were mixed in nitrogen balance using the HOVAGAS mixer and gas mixtures were directed into the cell at flow rates from 1 to 5 l/min. For long-term stability tests the cell was filled with a known gas mixture and sealed. The results were converted to the gas concentration unit %v·m. For zero H_2 measurements the cell was removed from the test bench and ambient air was measured.

Figure 7(a) plots the obtained 2*f* WMS signals for 0.5, 0.2 and 0.1 %v of H_2 in nitrogen for an optical pathlength of 1 meter. The signal for zero hydrogen concentration was recorded when sensor measured through ambient air. Each signal was acquired during 1 second as a result of averaging of 150 laser wavelength scans. To improve sensitivity the signals can further be processed using e.g. wavelet denoising or band-pass filtering. Here, convolution with a Mexican hat wavelet function was used. The width of the function was chosen to match the width of the H_2 absorption feature. Figure 7(b) demonstrates the improved SNR after the convolution. The baseline slope and high frequency noise components were removed. It is seen that the peak from 0.1 %v·m is clearly distinguishable from the noise level, which indicates that the obtained sensitivity of the sensor to the fractional absorbance is better than 2×10^{-6}. The SNR approach was applied to estimate the LOD of the sensor. In this approach LOD corresponds to the concentration level at which the measured signal (peak-to-peak) reaches 3 times the signal noise (peak-to-peak) of the baseline. By using this criteria LOD of the H_2 sensor was estimated to be 0.1 %v·m for 1 s integration time.

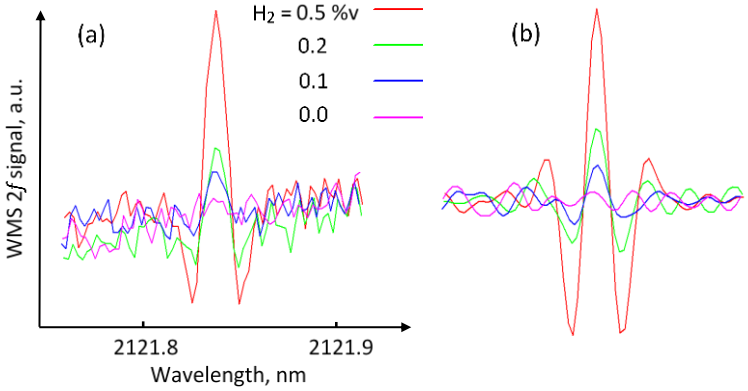

Figure 7. (a) 2*f* WMS sensor signals for three different H_2 concentrations and one zero signal. Corresponded concentrations at 1 meter of optical pathlength are 0.5, 0.2, 0.1 %v. The zero signal was recorded in ambient air; (b) The signals after convolution with the matched Mexican hat wavelet function demonstrating the improved SNR.

To examine the capability of the sensor in terms of the measurement precision and the long-term stability, the sensor was installed on a cell to measure 1.0 %v·m H_2 in nitrogen and the data were logged over 500 min with 1 second resolution. Figure 8(a) shows the plot of the measured concentration. Along with stochastic noise an oscillating pattern can be observed which we attribute to optical fringes from the cell windows which were drifting due to the changing ambient temperature. The corresponding Allan deviation [31] (1σ) is plotted in Figure 8(b). The precision without averaging, i.e. with sensor update time of 1 s was 0.02 %v·m. The precision improved with averaging and after 20 s of averaging 0.005 %v·m was achieved. Between 1 and 10 min of averaging time the Allan deviation increased up to approximately 0.02 %v·m. This behavior can be attributed to combination of etalon noise from the cell windows and etalon noise from the sensor optical system. Thus, long term drift and short-term (1 s) precision are both at about the same value of 0.02 %v·m, which demonstrates excellent overall performance of the sensor.

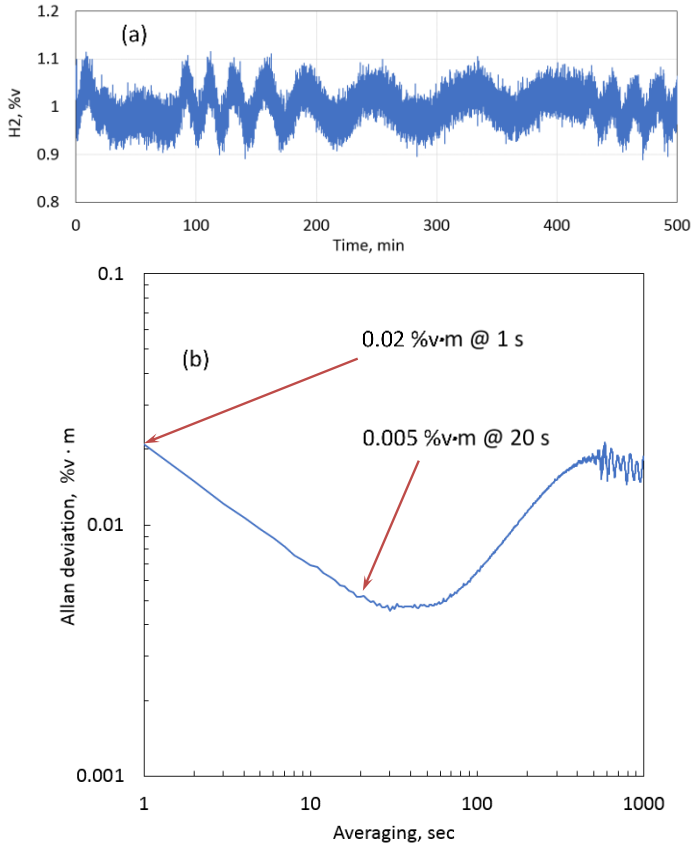

Figure 8. a) Long term measurements of 1 %v H_2 over 1 meter with 1 s update time; b) Allan deviation of the sensor measurements (1σ). Demonstrated precision is 0.02 % v·m at 1 s (no averaging) and 0.005 % v·m with 20 s averaging.

For linearity evaluation a HOVAGAS gas mixing system was used to generate H_2 concentrations stepwise down from 10 %v to 0.1 %v by diluting pure hydrogen in nitrogen base. Each concentration was measured during about 4 min. Figure 9(a) shows the recorded measurements. The measurements for each concentration step were averaged and plotted in Figure 9(b) against the nominal concentration set in the gas mixer software. The linear fit has a slope well within 0.5% of the sensor range and an *R*-square value of 0.9998 confirms the excellent linearity of the H_2 sensor.

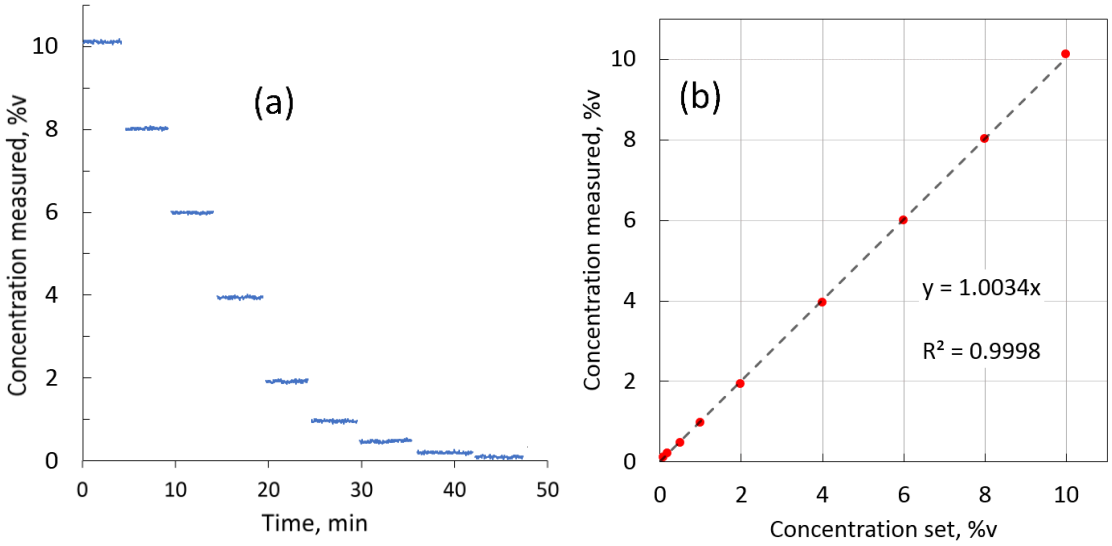

Figure 9. a) Sensor response to different H_2 concentrations (10.0, 8.0, 6.0, 4.0, 2.0, 1.0, 0.5, 0.2, 0.1 %v) in the 0.7 m cell; b) Plot of the measured concentration as a function of the concentration set in the gas mixer and a linear fit.

6. Conclusions

A TDLAS sensor was developed for industrial in-situ and non-contact measurements of hydrogen. The sensor uses a well-proven LaserGas™ II platform by NEO Monitors AS and a 2122 nm DFB laser. The selected quadrupole absorption line of H_2 was characterized in terms of collisional broadening and narrowing effects. The line exhibits sub-doppler width in wide ranges of pressures not only for pure hydrogen but also for hydrogen in nitrogen and air balance. The broadening and narrowing coefficients for nitrogen and air were obtained by fitting the measured linewidth to the calculated linewidth from the Hartmann-Tran profile. The performance of the sensor was evaluated. The measurement precision of 0.02 %v H_2 for just 1 meter of the absorption pathlength was achieved for 1 s of the integration time. Using the SNR approach the corresponding LOD was estimated to be 0.1 %v of H_2 in air which is sufficient for safety applications. By increasing the absorption pathlength and/or integration time the performance of the sensor can further be improved, which should widen the applicability of the sensor also for applications with sub-% H_2 levels.

Author Contributions: Conceptualization, V.A.; Methodology, V.A. and O.B.; Investigation, V.A. and O.B.; Software, J.W. and P.G.; Formal analysis, V.A. and J.W.; Writing—original draft preparation, V.A.; Writing—review and editing, P.G.; Project administration, V.A., P.G. and K.G.P.; Supervision, K.G.P.

Funding: This research received no external funding.

Acknowledgments: In this section you can acknowledge any support given which is not covered by the author contribution or funding sections. This may include administrative and technical support, or donations in kind (e.g., materials used for experiments).

Conflicts of Interest: The authors declare no conflict of interest.

References

1. Jain, I. P. Hydrogen the Fuel for 21st Century. International Journal of Hydrogen Energy 2009, 34 (17), 7368–7378. https://doi.org/10.1016/j.ijhydene.2009.05.093.
2. Buttner, W. J.; Post, M. B.; Burgess, R.; Rivkin, C. An Overview of Hydrogen Safety Sensors and Requirements. *International Journal of Hydrogen Energy* **2011**, *36* (3), 2462–2470. https://doi.org/10.1016/j.ijhydene.2010.04.176.
3. Hübert, T.; Boon-Brett, L.; Black, G.; Banach, U. Hydrogen Sensors – A Review. *Sensors and Actuators B: Chemical* **2011**, *157* (2), 329–352. https://doi.org/10.1016/j.snb.2011.04.070.

4. Gordon, I. E.; Rothman, L. S.; Hill, C.; Kochanov, R. V.; Tan, Y.; Bernath, P. F.; Birk, M.; Boudon, V.; Campargue, A.; Chance, K. V.; et al. The HITRAN2016 Molecular Spectroscopic Database. *Journal of Quantitative Spectroscopy and Radiative Transfer* **2017**, *203*, 3–69. https://doi.org/10.1016/j.jqsrt.2017.06.038.
5. O'Keefe, A.; Deacon, D. A. G. Cavity Ring-down Optical Spectrometer for Absorption Measurements Using Pulsed Laser Sources. *Review of Scientific Instruments* **1988**, *59* (12), 2544–2551. https://doi.org/10.1063/1.1139895.
6. Campargue, A.; Kassi, S.; Pachucki, K.; Komasa, J. The Absorption Spectrum of H2: CRDS Measurements of the (2-0) Band, Review of the Literature Data and Accurate Ab Initio Line List up to 35 000 Cm−1. *Phys. Chem. Chem. Phys.* **2011**, *14* (2), 802–815. https://doi.org/10.1039/C1CP22912E.
7. O'Keefe, A. Integrated Cavity Output Analysis of Ultra-Weak Absorption. *Chemical Physics Letters* **1998**, *293* (5), 331–336. https://doi.org/10.1016/S0009-2614(98)00785-4.
8. Baer, D. S.; Paul, J. B.; Gupta, M.; O'Keefe, A. Sensitive Absorption Measurements in the Near-Infrared Region Using off-Axis Integrated-Cavity-Output Spectroscopy. *Appl Phys B* **2002**, *75* (2), 261–265. https://doi.org/10.1007/s00340-002-0971-z.
9. Morville, J.; Kassi, S.; Chenevier, M.; Romanini, D. Fast, Low-Noise, Mode-by-Mode, Cavity-Enhanced Absorption Spectroscopy by Diode-Laser Self-Locking. *Appl. Phys. B* **2005**, *80* (8), 1027–1038. https://doi.org/10.1007/s00340-005-1828-z.
10. Cassidy, D. T.; Reid, J. Atmospheric Pressure Monitoring of Trace Gases Using Tunable Diode Lasers. *Appl. Opt., AO* **1982**, *21* (7), 1185–1190. https://doi.org/10.1364/AO.21.001185.
11. Werle, P.; Slemr, F.; Maurer, K.; Kormann, R.; Mücke, R.; Jänker, B. Near- and Mid-Infrared Laser-Optical Sensors for Gas Analysis. *Optics and Lasers in Engineering* **2002**, *37* (2), 101–114. https://doi.org/10.1016/S0143-8166(01)00092-6.
12. Hanson, R. K. Applications of Quantitative Laser Sensors to Kinetics, Propulsion and Practical Energy Systems. *Proceedings of the Combustion Institute* **2011**, *33* (1), 1–40. https://doi.org/10.1016/j.proci.2010.09.007.
13. Lackner, M. Tunable Diode Laser Absorption Spectroscopy (TDLAS) in the Process Industries – A Review. *Reviews in Chemical Engineering* **2011**, *23* (2), 65–147. https://doi.org/10.1515/REVCE.2007.23.2.65.
14. Geiser, P. New Opportunities in Mid-Infrared Emission Control. *Sensors* **2015**, *15* (9), 22724–22736. https://doi.org/10.3390/s150922724
15. Geiser, P.; Avetisov, V.; Espinoza-Nava, L.; Menegazzo, N.; Kaspersen, P. Continuous Emission Monitoring of Tetrafluoromethane Using Quantum Cascade Lasers. *Photonics* **2016**, *3* (2), 16. https://doi.org/10.3390/photonics3020016 (1)
16. Chao, X.; Jeffries, J. B.; Hanson, R. K. Absorption Sensor for CO in Combustion Gases Using 2.3 μm Tunable Diode Lasers. *Meas. Sci. Technol.* **2009**, *20* (11), 115201. https://doi.org/10.1088/0957-0233/20/11/115201.
17. NEO Monitors. Available online: http://neomonitors.com (accessed on 31 October 2019).
18. Bomse, D. S.; Stanton, A. C.; Silver, J. A. Frequency Modulation and Wavelength Modulation Spectroscopies: Comparison of Experimental Methods Using a Lead-Salt Diode Laser. *Appl. Opt., AO* **1992**, *31* (6), 718–731. https://doi.org/10.1364/AO.31.000718.
19. Silver, J. A. Frequency-Modulation Spectroscopy for Trace Species Detection: Theory and Comparison among Experimental Methods. *Appl. Opt., AO* **1992**, *31* (6), 707–717. https://doi.org/10.1364/AO.31.000707.
20. Schilt, S.; Thévenaz, L.; Robert, P. Wavelength Modulation Spectroscopy: Combined Frequency and Intensity Laser Modulation. *Appl. Opt., AO* **2003**, *42* (33), 6728–6738. https://doi.org/10.1364/AO.42.006728.
21. Klein, A.; Witzel, O.; Ebert, V. Rapid, Time-Division Multiplexed, Direct Absorption- and Wavelength Modulation-Spectroscopy. *Sensors* **2014**, *14* (11), 21497–21513. https://doi.org/10.3390/s141121497.
22. Ghorbani, R.; Schmidt, F. M. ICL-Based TDLAS Sensor for Real-Time Breath Gas Analysis of Carbon Monoxide Isotopes. *Opt. Express, OE* **2017**, *25* (11), 12743–12752. https://doi.org/10.1364/OE.25.012743.
23. Zheng, K.; Zheng, C.; He, Q.; Yao, D.; Hu, L.; Zhang, Y.; Wang, Y.; Tittel, F. K. Near-Infrared Acetylene Sensor System Using off-Axis Integrated-Cavity Output Spectroscopy and Two Measurement Schemes. *Opt. Express, OE* **2018**, *26* (20), 26205–26216. https://doi.org/10.1364/OE.26.026205.
24. Kassi, S.; Campargue, A. Electric Quadrupole Transitions and Collision-Induced Absorption in the Region of the First Overtone Band of H2 near 1.25μm. *Journal of Molecular Spectroscopy* **2014**, *300*, 55–59. https://doi.org/10.1016/j.jms.2014.03.022.
25. Ngo, N. H.; Lisak, D.; Tran, H.; Hartmann, J.-M. An Isolated Line-Shape Model to Go beyond the Voigt Profile in Spectroscopic Databases and Radiative Transfer Codes. *Journal of Quantitative Spectroscopy and Radiative Transfer* **2013**, *129*, 89–100. https://doi.org/10.1016/j.jqsrt.2013.05.034.

26. Rautian, S. G.; Sobel'man, I. I. The Effect of Collisions on the Doppler Broadening of Spectral Lines. *Sov. Phys. Usp.* **1967**, *9* (5), 701. https://doi.org/10.1070/PU1967v009n05ABEH003212.
27. Galatry, L. Simultaneous Effect of Doppler and Foreign Gas Broadening on Spectral Lines. *Phys. Rev.* **1961**, *122* (4), 1218–1223. https://doi.org/10.1103/PhysRev.122.1218.
28. Wcisło, P.; Gordon, I. E.; Tran, H.; Tan, Y.; Hu, S.-M.; Campargue, A.; Kassi, S.; Romanini, D.; Hill, C.; Kochanov, R. V.; et al. The Implementation of Non-Voigt Line Profiles in the HITRAN Database: H2 Case Study. *Journal of Quantitative Spectroscopy and Radiative Transfer* **2016**, *177*, 75–91. https://doi.org/10.1016/j.jqsrt.2016.01.024. (1)
29. Reid, J.; Labrie, D. Second-Harmonic Detection with Tunable Diode Lasers — Comparison of Experiment and Theory. *Appl. Phys. B* **1981**, *26* (3), 203–210. https://doi.org/10.1007/BF00692448.
30. Chakraborty, A. L.; Ruxton, K.; Johnstone, W.; Lengden, M.; Duffin, K. Elimination of Residual Amplitude Modulation in Tunable Diode Laser Wavelength Modulation Spectroscopy Using an Optical Fiber Delay Line. *Opt. Express, OE* **2009**, *17* (12), 9602–9607. https://doi.org/10.1364/OE.17.009602.
31. Werle, P. Accuracy and Precision of Laser Spectrometers for Trace Gas Sensing in the Presence of Optical Fringes and Atmospheric Turbulence. *Appl. Phys. B* **2011**, *102* (2), 313–329. https://doi.org/10.1007/s00340-010-4165-9.